Article

Cell Host & Microbe

Conspecific versus heterospecific transmission shapes host specialization of the phyllosphere microbiome

Graphical abstract

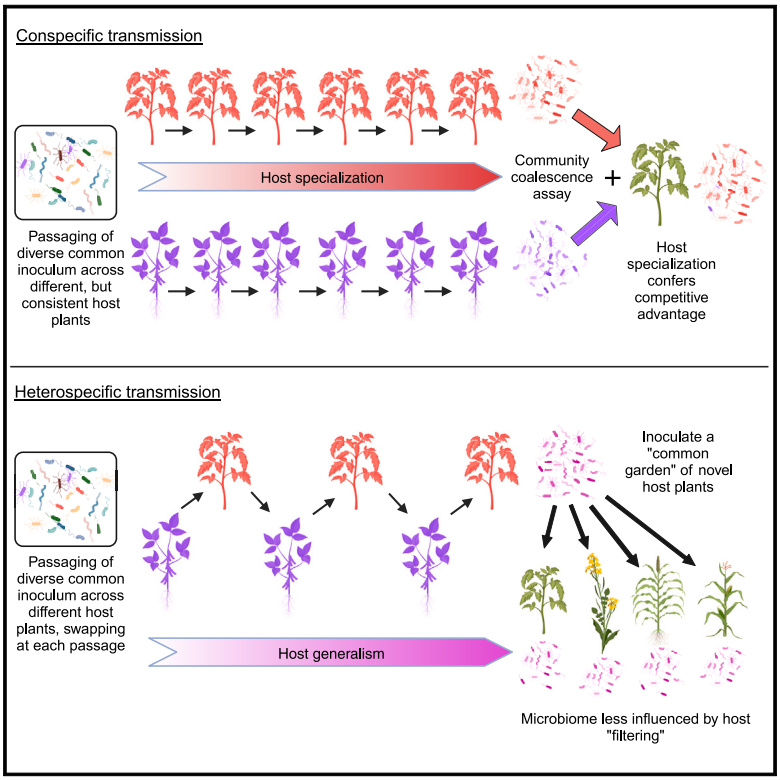

Highlights

- Host specialization of microbiome can occur via conspecific microbiome transmission
- Microbiome specialization occurs independent of host fitness or leaf transcription
- Heterospecific transmission drives microbiomes toward taxonomic homogenization
- Heterospecific transmission of microbiomes may confer host generalism

Authors

Kyle M. Meyer, Isabella E. Muscettola, Ana Luisa S. Vasconcelos, Julia K. Sherman, C. Jessica E. Metcalf, Steven E. Lindow, Britt Koskella

Correspondence

kmmeyer@berkeley.edu

In brief

Microbial transmission between hosts is known to have dramatic consequences for host-symbiont interactions. The question of whether this holds true for complex microbiomes remains largely unexplored. Meyer et al. manipulate plant microbiome transmission over multiple generations to show how microbiome host specialization and generalism can arise without impacting plant fitness or gene expression.

Meyer et al., 2023, Cell Host & Microbe *31*, 2067–2079
December 13, 2023 © 2023 The Authors. Published by Elsevier Inc.
https://doi.org/10.1016/j.chom.2023.11.002

CellPress

Cell Host & Microbe

CellPress
OPEN ACCESS

Article

Conspecific versus heterospecific transmission shapes host specialization of the phyllosphere microbiome

Kyle M. Meyer,[1,4,6,*] Isabella E. Muscettola,[1] Ana Luisa S. Vasconcelos,[1,2] Julia K. Sherman,[1] C. Jessica E. Metcalf,[3] Steven E. Lindow,[4] and Britt Koskella[1,5]

[1]Department of Integrative Biology, University of California, Berkeley, Berkeley, CA 94720, USA
[2]Department of Soil Science, College of Agriculture "Luiz de Queiroz", Universidade de São Paulo, Piracicaba 13418-900, Brazil
[3]Department of Ecology and Evolutionary Biology, Princeton University, Princeton, NJ 08544, USA
[4]Department of Plant and Microbial Biology, University of California Berkeley, Berkeley, CA 94720, USA
[5]Chan Zuckerberg Biohub, San Francisco, San Francisco, CA 94158, USA
[6]Lead contact
*Correspondence: kmmeyer@berkeley.edu
https://doi.org/10.1016/j.chom.2023.11.002

SUMMARY

In disease ecology, pathogen transmission among conspecific versus heterospecific hosts is known to shape pathogen specialization and virulence, but we do not yet know if similar effects occur at the microbiome level. We tested this idea by experimentally passaging leaf-associated microbiomes either within conspecific or across heterospecific plant hosts. Although conspecific transmission results in persistent host-filtering effects and more within-microbiome network connections, heterospecific transmission results in weaker host-filtering effects but higher levels of interconnectivity. When transplanted onto novel plants, heterospecific lines are less differentiated by host species than conspecific lines, suggesting a shift toward microbiome generalism. Finally, conspecific lines from tomato exhibit a competitive advantage on tomato hosts against those passaged on bean or pepper, suggesting microbiome-level host specialization. Overall, we find that transmission mode and previous host history shape microbiome diversity, with repeated conspecific transmission driving microbiome specialization and repeated heterospecific transmission promoting microbiome generalism.

INTRODUCTION

Transmission mode, i.e., the means by which microorganisms move between hosts, has the potential to shape host-microbe interactions over both short, microevolutionary, and longer, macroevolutionary, timescales.[1,2] Both theory and empirical evidence suggest that strict vertical (parent-to-offspring) transmission of individual microbial symbionts or pathogens can drive highly specialized adaptations for the symbiont, including genome reduction and streamlined metabolic capability,[3] as well as reduced virulence.[4,5] Similarly, transmission between conspecific (same species) hosts can drive the formation of mutualistic relationships, whereby the fitness of both participants increases through the shared benefits of cooperation.[6] On the other hand, horizontal, or heterospecific, transmission (i.e., between unrelated hosts) can drive increased virulence in pathogens[7] and may promote a "jack-of-all-trades, master of none" strategy in symbionts, whereby symbionts are less beneficial to host fitness,[6] less likely to gain host-specific adaptations, and more likely to return to autonomy.[8] Importantly, much of this framework has centered on pairwise interactions, and a considerable gap remains regarding whether transmission mode may also shape the local adaptation of the complex consortia of microorganisms residing in or on a host, known as the microbiome.

Aboveground plant tissue, also known as the phyllosphere, harbors a distinct microbiome comprising bacteria, fungi, and viruses.[9,10] Phyllosphere microbiomes are implicated in multiple facets of plant health, including disease resistance,[11–13] auxin production,[14] and primary productivity.[15] These microbial communities assemble primarily *de novo* at seed germination or leaf emergence and tend to follow distinct assembly patterns depending on the host plant species.[16] These host species identity effects arise on leaf surfaces through ecological (host) filtering resulting from different chemical and physical features of the host,[17,18] as well as immune activity,[19,20] molecular signaling,[9] and tissue/barrier formation.[21] Importantly, such filtering effects depend on the diversity of microbial taxa arriving on the leaf and are thus reliant on the process of dispersal.[22]

A major source of microbial dispersal into the phyllosphere is the nearby vegetation,[23] and the species identity, size, and environmental context of surrounding vegetation have been shown to impact microbiome assembly.[24–26] In low diversity plant

This is an open access article under the CC BY-NC license (http://creativecommons.org/licenses/by-nc/4.0/).

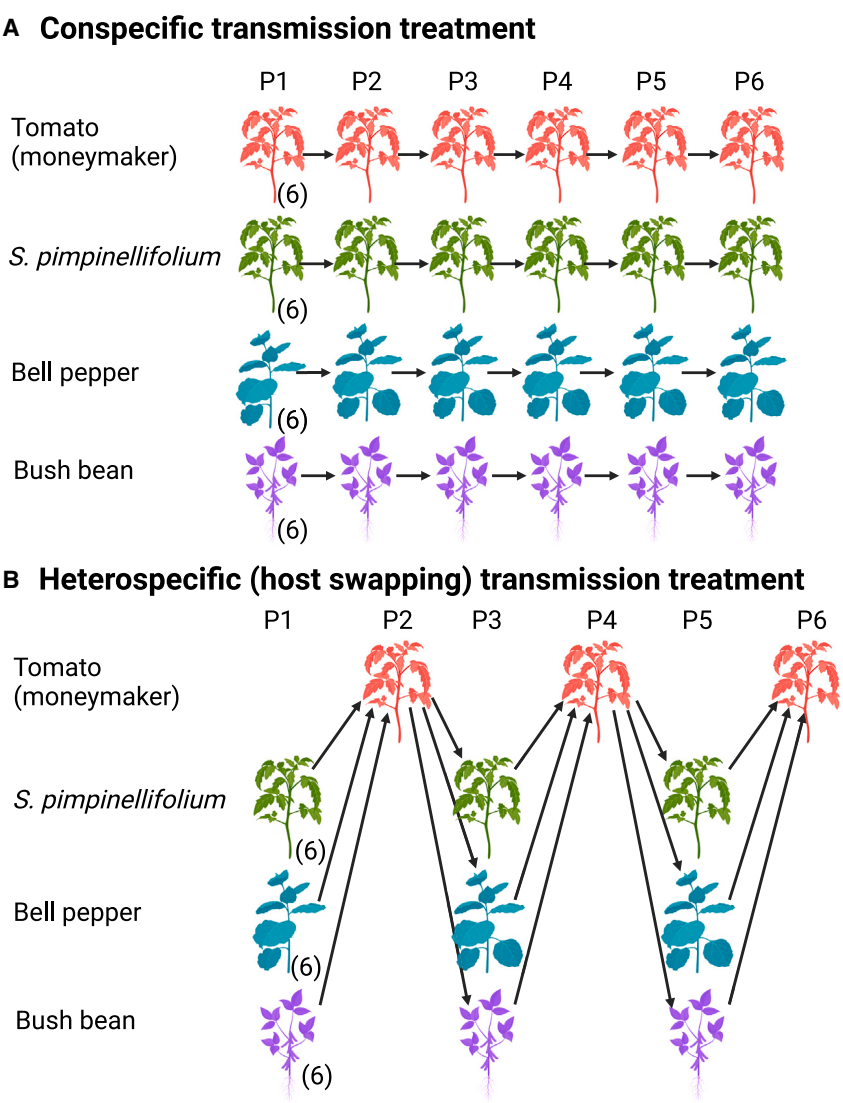

Figure 1. Experimental design of the main passaging experiment where a diverse microbial inoculum was sprayed onto 4 species of plant (moneymaker tomato, *Solanum pimpinellifolium*, bell pepper, and bush bean), allowed to establish and grow, and then be harvested to act as inoculum for the subsequent passage (P2–P6)

(A) Conspecific (same species) transmission treatment whereby replicate microbiome lineages are passaged only on plants of the same species.

(B) Heterospecific, or host swapping, transmission treatment whereby replicate lineages start on *S. pimpinellifolium*, bell pepper, or bush bean host plants but passage back and forth between tomato hosts and host species of origin. In both cases, each replicate line remained independent across passages (i.e., microbiomes from one individual plant were used as inoculum for one plant in the next passage).

communities, we might expect transmission among related plants to be more likely than among unrelated plants, and this consistent plant-driven selective pressure, known as the ecological/plant-filtering effect, could promote host specialization of microbiomes. In contrast, frequent transmission among different plant species, as might be the norm in higher diversity plant communities, may disrupt microbiome specialization and instead select for taxa that are able to persist through multiple sets of host filters, driving increased microbiome generalism. Better understanding the means by which specialization or generalism arise could inform new strategies in sustainable agriculture, conservation, and microbiome engineering.[27–32] The longer-term consequences of such differences in transmission could also shed light on the formation or maintenance of symbiotic relationships over evolutionary time.

To better understand how microbiome transmission might shape host specialization, we experimentally passaged a diverse microbial community initially derived from field-grown tomato plants on either conspecific (one of the four plant species consistently) or heterospecific (alternating between tomato and each of the other three species at each passage) plant hosts. We used 16S rRNA gene amplicon sequencing to track microbiome assembly across treatments over six plant passages and then further explored specialization of the microbiomes in two follow-up experiments—one that applied experimental community coalescence to directly test for microbiome host specialization and another in which microbiomes were transplanted onto novel hosts in a "common garden experiment" to test for microbiome host generalism. In both the primary passaging experiment and follow-up studies, we find clear but nuanced evidence of microbiome specialization, as well as clear plant-filtering effects upon this common pool of microbial taxa. These findings make clear that by altering the species pool on which host selection acts, transmission mode can impact the outcome of microbiome assembly and shape the prospects for host specialization of the microbiome.

RESULTS

Microbiomes were passaged conspecifically (on a single host species) or heterospecifically (host swapped) for 6 experimental time points (Figure 1). After sample processing and DNA extraction, all samples from the passaging experiment (n = 300) yielded high-quality sequences. The dataset contained 7,452,252 observations of 3,227 amplicon sequence variants (ASVs), 1,842 of which had >10 occurrences, and 539 of which had >100 occurrences. The original taxonomic pool from which the inoculum came contained a minimum of 550 ASVs (at detection levels) from Davis and 139 from Encinitas, with 40 ASVs shared between the sites. Microbiomes from the blank inoculum control plants meant to survey taxa arriving from the greenhouse environment collectively contained 1,512 ASVs, 1,073 of which were detected only once, and 163 of which were detected in the initial inoculum.

Table 1. Phyllosphere bacterial assemblages vary by passage number, host species identity, transmission mode, block, and a species identity-by-transmission mode interaction

–	*df*	Pseudo-*f*	R^2	p	Significance
Passage	5	36.9	0.384	0.001	***
Host species	3	11.7	0.073	0.001	***
Transmission mode	1	1.1	0.002	0.001	***
Block	1	15.7	0.033	0.001	***
Host species × transmission mode	3	2.2	0.013	0.03	*

Results of a PERMANOVA on Bray-Curtis dissimilarities of bacterial communities, with line ID specified as strata. Term order is as follows: passage number, species identity, transmission mode, and experimental block.

Throughout the six experimental passages, taxa from the Encinitas (early growing season) collection on average comprised a higher proportion of read counts in the resulting experimental microbiomes than the taxa from the Davis (late growing season) collection (Figure S1A), and the taxa shared among the two collection sites tended to comprise roughly one-quarter of a microbiome's sequencing reads (Figure S1B). At the end of the final passage, phyllosphere microbiome densities ranged from 1.3×10^5 to 3.2×10^6 (median = 9.5×10^5) bacterial cells per g leaf material and did not significantly differ by host or transmission group (Tukey honest significance test [HSD] $p > 0.1$).

Experimental passage, host species identity, and transmission mode shape phyllosphere bacterial composition

Phyllosphere communities across the 252 treatment samples were dominated by taxa affiliated with the genera *Exiguobacterium*, *Pantoea*, *Sphingomonas*, *Pseudomonas*, and *Klebsiella* (Figures S2A–S2C). The PERMANOVA model explaining Bray-Curtis dissimilarity among these samples revealed statistically significant effects of passage time point (1–6), the species identity of the host plant, transmission mode (conspecific versus host swapping transmission), experimental block, and an interaction between host species identity and transmission mode (Figure S3A; Table 1). In other words, the effects of transmission mode (conspecific or host swapping) depend on the host plant species between which transmission takes place.

To gain a better understanding of whether the observed effect of passage time point is driven by seasonality, we examined the microbiomes that developed on the seasonality control plants that were treated with the initial inoculum at time points 2–6. A difference in community structure across passage time points was observed in these microbiomes (P2–P6, PERMANOVA $R^2 = 0.647$, $p < 0.001$); however, when compared with the passage 1 tomato microbiomes, there were no significant pairwise differences in composition (pairwise PERMANOVA $p > 0.05$) for any of the passages, suggesting relative similarities in initial host filtering through time from a common pool of microorganisms.

Microbiome richness steadily declines under host selection

The goal of the passaging experiment was to observe any microbiome community-level responses to host-imposed selection. As such, we predicted continuous loss of taxonomic diversity over time and expect the differences in taxa lost across independent lines to indicate stochasticity in this process, whereas the concerted loss across lines to indicate more deterministic processes. Across all lines, ASV richness levels declined over time ($F_{5, 252} = 32.01$, $p < 0.001$) and were influenced by host species identity ($F_{3, 252} = 10.15$, $p < 0.001$), with no effect of con- versus hetero-specific transmission ($F_{1, 252} = 0.52$, $p = 0.477$), and no interactions therein (Figure 2A). Overall, the 6 experimental passages resulted in microbiomes with roughly 2-fold lower richness levels at passage 6 relative to passage 1. At passage 6, all treatments were roughly equivalent in richness, but a trending effect of transmission mode could be detected ($F_{1, 42} = 3.92$, $p = 0.056$) wherein conspecifically transmitted groups had slightly higher richness than host swapping groups.

To examine phylogenetic clustering across plant species and transmission modes, we generated a phylogenetic tree comprising all bacterial ASVs from the experiment to test whether co-occurring taxa within a given microbiome/treatment are more closely related than expected by chance. Evidence for such phylogenetic clustering would consist of a negative standardized effect size of the mean pairwise distance (MPD SES) between pairs of co-occurring taxa. MPD SES values are significantly impacted by passaging time point ($F_{5, 239} = 15.47$, $p < 0.001$), host species identity ($F_{3, 239} = 56.57$, $p < 0.001$), transmission mode ($F_{1, 239} = 6.73$, $p < 0.05$), and a host-by-transmission mode interaction ($F_{3, 239} = 10.16$, $p < 0.001$). MPD SES values are consistently negative for the tomato, *Solanum pimpinellifolium*, and pepper conspecific transmission lines (Figure 2B, left), suggesting that selection for phylogenetically conserved traits in the microbiome had occurred. Lines that were swapped between these hosts were also persistently phylogenetically clustered throughout the experiment (Figure 2B, right). In contrast, lines passaged only on bean exhibited phylogenetic clustering at passage 1 but then trended toward positive values, suggesting phylogenetic overdispersion. The lines that alternated between bean and tomato also trended toward phylogenetic overdispersion when on bean hosts at passage 3.

Host species identity effects persist through conspecific transmission but decline under heterospecific transmission

To test whether transmission mode impacted the host species identity effects of microbiomes at each passage, we excluded the tomato conspecific lines to enable an even comparison of the 3 host swapping groups and their 3 conspecific transmission counterparts. At each passage time point, conspecific transmission lines exhibited statistically significant (i.e., $p_{adj} < 0.05$) host species identity effects, with effect sizes ranging from $R^2 = 0.35$ to 0.45 and fluctuating over time (Figure 3A). In contrast, host species identity effects in the heterospecific transmission lines exhibited a monotonic decrease over the 3 time points when they were on their focal host (i.e., not tomato; P1, P3, and P5). In other words, each time the heterospecific transmission lines transmitted back to their host species of origin, they were found to be less differentiable across host species.

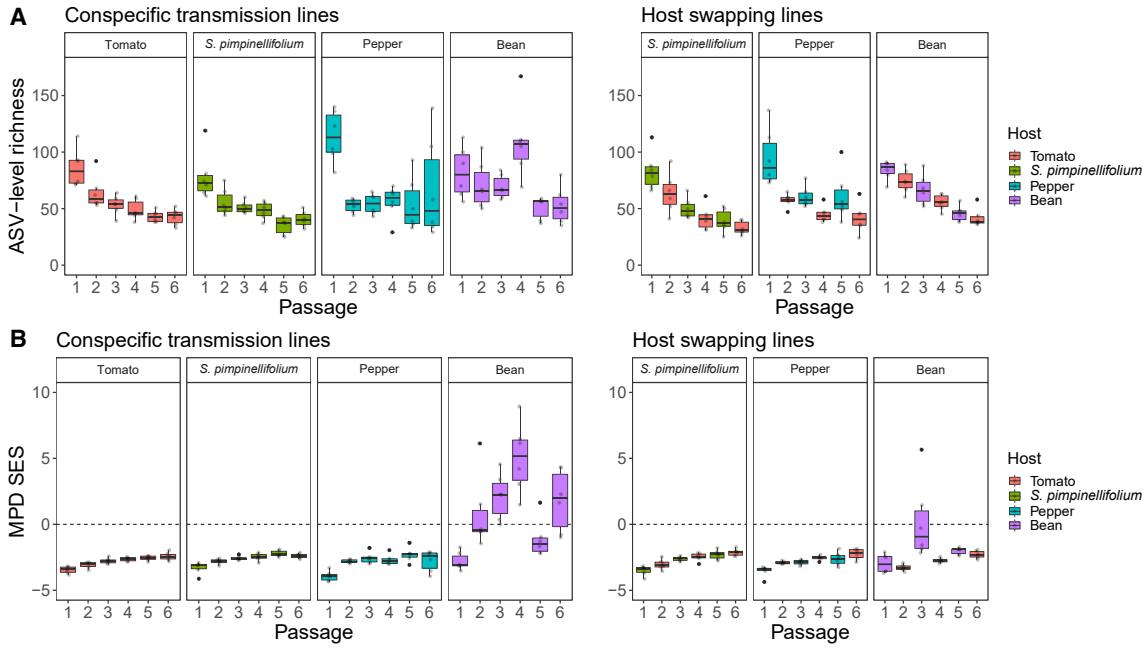

Figure 2. Experimental passaging, host selection, and transmission mode shape phyllosphere microbiome richness and phylogenetic structure

(A) ASV-level richness (y axis) decreases over 6 experimental passages (x axis). Panels on the left represent the conspecific transmission treatments, panels on the right represent the host swapping treatments, with box colored by host species identity.

(B) Phylogenetic clustering, represented by the standardized effect size of the mean pairwise distance (MPD SES, y axis) of conspecific (left) and host swapping (right) microbiome transmission treatments. SES = $(MPD_{obs} - MPD_{null})/SD(MPD_{null})$. Values below 0 (indicated by dashed line) suggest phylogenetic clustering where co-occurring taxa are more closely related than the null expectation (where taxa are drawn at random from the species pool), whereas values above 0 suggest phylogenetic overdispersion where co-occurring taxa are more distantly related than the null expectation. The bottom and top edges of boxes in A and B represent the 25th and 75th percentile, and the line within the box indicates the median. The box whiskers represent the range of data, excluding outliers, that fall more than 1.5 times the interquartile range below the first quartile or above the third quartile.

Previous host association leaves a discernible signal in microbiome structure despite host selection

At passages 2, 4, and 6, when host swapping microbiome lines were all on tomato hosts, we asked whether each line's previous host association left a discernible signal in the microbiome structure. None of the host swapping lines differed from the conspecifically transmitted tomato lines at passages 2, 4, or 6 (pairwise PERMANOVA $p_{adj} > 0.1$ for all comparisons), suggesting strong effects of host filtering by tomato plants. Despite this evidence for strong host filtering, the effect of previous host species identity was consistently detectable at each of these passages (passage 2: $R^2 = 0.30$, $p_{adj} = 0.003$, passage 4: $R^2 = 0.18$, $p_{adj} = 0.04$, and passage 6: $R^2 = 0.21$, $p_{adj} = 0.04$, Figure S3B), suggesting that the pool of microbial transplants had been sufficiently shaped by the previous host association to impact the outcome of assembly on tomato hosts.

Co-occurrence network structure is shaped by inter-host transmission

We next test the hypothesis that the selection imposed on microbiomes through successive passaging alters the connectivity of microbiome co-occurrence networks and that the two forms of transmission uniquely shape microbiome networks. We focus specifically on the following two network attributes: number of edges (i.e., connections between nodes, reflecting how many other ASVs a focal ASV co-occurs with) and clustering coefficient (i.e., how connected the edges of a node are with each other). At passage 6, the resultant microbiome network structures differ by transmission mode. In all three cases, the networks of the host swapping transmission groups have a higher clustering coefficient than their conspecific transmission counterparts (Figure 3B). In other words, in these host swapping networks, the ASVs to which a focal ASV (node) is connected tend to be more connected with each other, forming more network clusters (Figure S4A). By contrast, in all three cases, the networks of the conspecific transmission groups have a higher number of total edges (i.e., links) and number of nodes than their host swapping counterparts (Figures 3C and S4B). If we divide the edges into positive (persistent co-occurrence) and negative (persistent lack of co-occurrence) associations, we first see that the vast majority of network edges at passage 6 are positive (range of positive edges: 87–2,545, median = 270.5 versus range of negative edges 0–40, median = 0), and second that similar to the total edges, the positive edges are consistently higher in the conspecific lines relative to their host swapping counterparts. There are no negative edges for groups involving *S. pimpinellifolium* and pepper (i.e., <1), but for groups involving bean, the number of negative edges in host swap lines is 4.4 ± 0.6 compared with 20.7 ± 2.8 in conspecific lines. Thus, it appears that the two transmission modes impose different selective pressures on

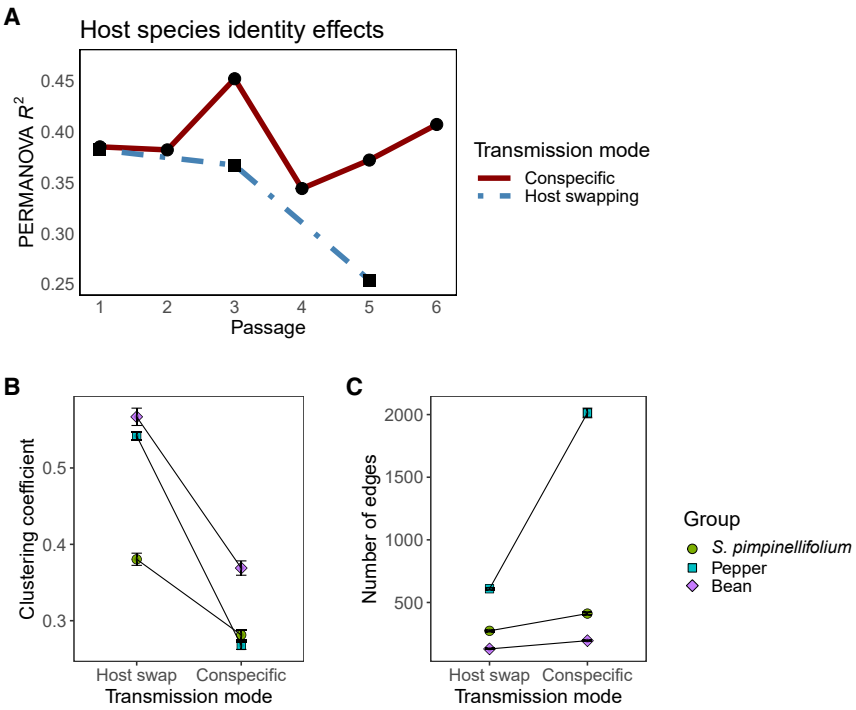

Figure 3. Phyllosphere microbiome composition and co-occurrence network structure are shaped by transmission mode

(A) Host species identity effects (y axis) on phyllosphere bacterial microbiomes are relatively constant over passage time point (x axis) for conspecific transmission mode (red solid line), whereas effects decrease in host swapping lines (dot-dash blue line). y axis is the PERMANOVA R^2 value tested on Bray-Curtis community dissimilarities with term order: host species identity and block. Statistical significance cutoff is $p < 0.05$, after accounting for multiple hypothesis tests using the Benjamini-Hochberg procedure. All points represent statistically significant effects. Note that tomatoes have been removed to make for an even comparison with host swap lines, and that host species identity effects cannot be assessed for host swap lines at passages 2, 4, and 6, when they are all on tomato.

(B) Co-occurrence network clustering coefficient (y axis) computed from replicate microbiome lines, separated by transmission mode (x axis) and host group (point shape and color).

(C) Co-occurrence network number of statistically significant edges (y axis) computed from replicate microbiome lines, separated by transmission mode (x axis) and host group (point shape and color). For (B) and (C), error bars represent 95% confidence intervals from 100 bootstrap iterations in which the community was rarefied and the networks were computed.

the microbiome co-occurrence networks, with host swapping lines exhibiting more clustering and conspecific transmission exhibiting more total positive associations.

More taxa differentially enriched in host swap lines relative to conspecific lines

We next ask whether the two transmission modes enrich for different taxa—for example, as a result of host specialization or network restructuring. We use a Bayesian implementation of logistic regression with binomial distribution on ASV presence/absence to assess differential establishment among transmission treatments. At the final time point, when we examine the pepper-associated lines, we identify 29 ASVs belonging to 14 bacterial genera (11 families, Table S1) that are more likely to establish on the host swapping lines, whereas no ASVs are more likely to establish on the conspecific lines. Similarly, for the bean-associated groups, we find 2 ASVs from different families (Table S1) that are more likely to establish on the host swapping lines and no taxa more likely to establish on conspecific lines. One of these ASVs (belonging to the Erwiniaceae family with no genus-level taxonomy) is enriched in both pepper and bean host swapping groups. This approach does not identify any ASVs that are differentially established in either of the *S. pimpinellifolium* groups. Since the host swapping lines had their final passage on tomato hosts, we further ask whether any differential patterns of presence/absence can be observed relative to the tomato conspecific transmission groups. Indeed, 4 ASVs associated with 3 genera are identified as more likely to establish on tomato conspecific lines relative to pepper host swap lines (Table S1). Furthermore, 3 of these ASVs are identified as more likely to be on tomato relative to the bean host swap lines (Table S1). There are no taxa differentially present between *S. pimpinellifolium* host swap lines and tomato conspecific lines, and there are no taxa identified as more likely to establish on the host swapping lines relative to conspecific tomato lines.

Evidence of microbiome host specialization using experimental community coalescence

To test whether conspecific transmission drives host specialization, we devised a community coalescence experiment using the conspecifically transmitted tomato, pepper, and bean microbiome lines resulting from passage 6. The six replicate lines for each host species group were combined and used to inoculate a new set of tomato hosts with equal densities of live bacterial cells from each source. Two community coalescence treatment groups were established by mixing equal ratios of live bacterial cells from tomato and pepper groups or tomato and bean groups (Figure 4A). Here, the expectation is that on a common host, microbiomes will compositionally segregate by their previous host association and that the coalescence treatments will more closely resemble the tomato microbiomes than the pepper or bean microbiomes due to the competitive advantage the tomato microbiomes would have gained through conspecific transmission.

Bacterial microbiomes of the treatment plants grew to greater densities than that attained on plants treated with the heat-killed inoculum and $MgCl_2$ controls (Tukey's HSD $p < 0.01$), with the exception of plants treated with a bean-derived inoculum, which grew to roughly 5× lower density than other treatment plants and statistically indistinguishable levels as the controls (Tukey's HSD $p > 0.1$; Figure 4B). All other treatment plants harbored statistically indistinguishable epiphytic densities (range: 1.7×10^5–1.3×10^6 bacterial cells per g plant material,

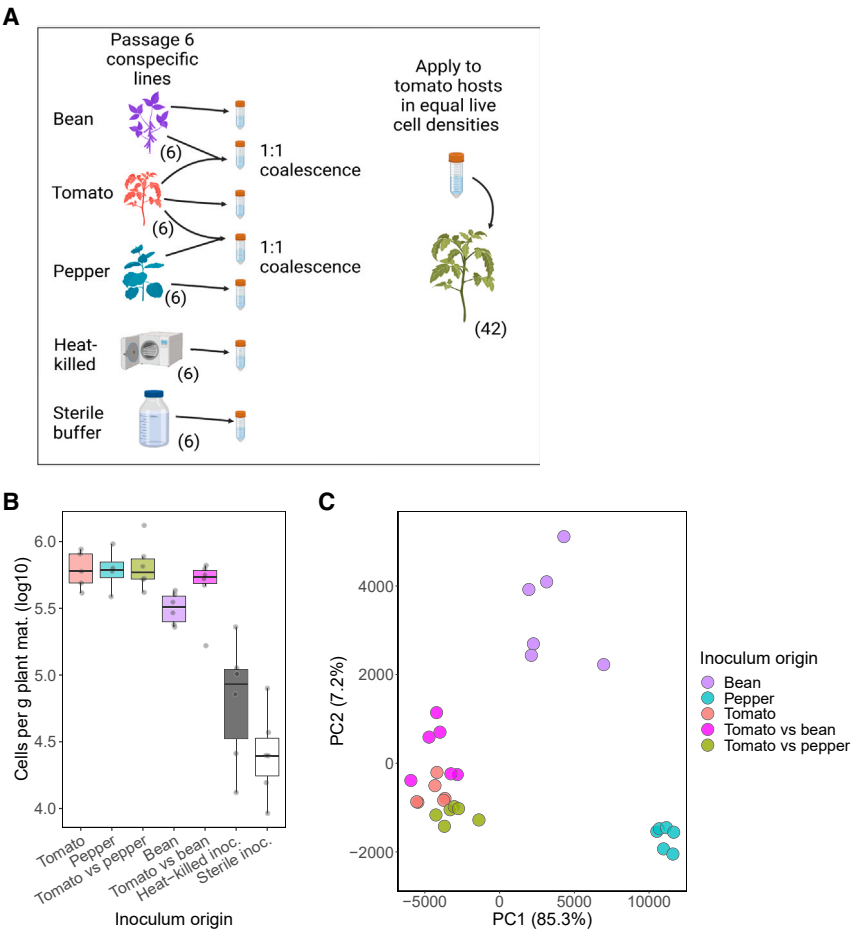

Figure 4. Conspecifically passaged lines show evidence of host specialization

(A) Schematic representation of experimental design in which microbial inocula of different transmission history origins were sprayed onto tomato hosts in equal densities of live cells three times. Inoculum origin is as follows: tomato (conspecifically passaged on tomato), pepper (conspecifically passaged on pepper), bean (conspecifically passaged on bean), tomato versus pepper (community coalescence treatment whereby equal densities of tomato and pepper inocula were combined then sprayed on at the same density as the other treatments), tomato versus bean (community coalescence with tomato and bean inocula), heat-killed inoculum, and sterile inoculum (10 mM $MgCl_2$).

(B) Bacterial microbiome densities (bacterial cells per g plant material) on a $\log_{10}$ scale (y axis), as measured by ddPCR of leaf wash, separated by microbiome treatment (x axis). The bottom and top edges of boxes indicate the 25th and 75th percentiles, respectively, and the line in the box represents the median. Box whiskers represent the data, excluding outliers, that fell more than 1.5 times the interquartile range below the first quartile or above the third quartile.

(C) Principal-component analysis of resultant bacterial microbiomes colored by their inoculum origin or coalescence treatment.

median: 6.0×10^5). The communities on tomato, pepper, and bean lines were significantly distinguishable in composition by their previous host association (Figure 4C; Table 2), suggesting a lingering differentiation driven by microbiome history. All treatment plants developed microbiomes that were significantly distinguishable in composition from the heat-killed and sterile inoculum controls (Figure S5A; Table S2).

We find support for our hypothesis that tomato microbiome members would come to dominate the pepper and bean microbiomes on a tomato host. The bean-tomato and the pepper-tomato coalescence treatments cluster more closely with the tomato group than the bean or pepper groups, respectively (Figure 4C). Pairwise PERMANOVA on Bray-Curtis dissimilarities reveals that the bean-tomato and tomato microbiomes were statistically indistinguishable (Table 2). The pepper-tomato coalescence and the tomato microbiomes are statistically discernible, but the effect size of these differences is smaller than that between the pepper-tomato and the pepper microbiomes (R^2 = 0.29 versus R^2 = 0.95, Table 2), suggesting a trend toward dominance of the tomato microbiome.

No effect of phyllosphere microbiome specialization on leaf transcriptional activity or tomato host fitness

We next asked whether the tomato-specialized microbiomes elicited discernable transcriptional responses in leaves compared with the other conspecific microbiome lines or control inocula. Leaves were sampled and flash frozen the day following inoculations 1 and 3 (weeks 1 and 3) of the specialization experiment and then subsequently processed for RNA extraction, cDNA sequencing, and differential gene expression analysis. Each of these samples yielded high-quality sequencing reads that were successfully mapped to the tomato genome. At both time points 1 and 2, we find no genes that are differentially expressed in the tomato microbiome-treated plants relative to plants treated with sterile $MgCl_2$ or with heat-killed bacterial inoculum. Next, we find no evidence for genes differentially expressed between the plants receiving the tomato microbiome and the bacterial inoculum from any of the other microbiome-treated plants. When we ordinate the RNA sequencing (RNA-seq) data along principle components 1 and 2, we see that the only factor driving a distinction of samples by their transcriptional profile is the time point at which they were sampled (i.e., week 1 versus week 3, PC1 $F_{1,7}$ = 268.9, $p < 0.001$, PC2 $F_{1,7}$ = 14.0, $p < 0.001$; Figure S5B), likely reflecting different development stages of the plants over the 2-week growth period. We thus conclude that microbiome-level specialization may take place on the leaf surface while not discernibly impacting leaf transcriptional activity.

Since repeated transmission among conspecific hosts has the potential to enrich for host beneficial or deleterious microbial taxa, we monitored the experimental plants for several indicators

CellPress
OPEN ACCESS

Table 2. Pairwise PERMANOVA table showing differences of Bray-Curtis dissimilarities between microbiomes differing in the host on which they were previously conspecifically passaged for 6 passages, prior to being inoculated on tomato hosts or combined in equal densities as a community coalescence assay

Pairwise PERMANOVA				
Comparison	R^2	*df*	*f*	p_{adj}
Tomato-pepper	0.933	1,10	141.5	0.006
Tomato-TP	0.289	1,10	4.07	0.006
Pepper-TP	0.947	1,10	179.94	0.004
Tomato-bean	0.759	1,10	31.62	0.004
Tomato-TB	0.092	1,10	1.02	0.435
Bean-TB	0.723	1,10	26.13	0.005
Pepper-bean	0.818	1,10	45.06	0.004
Pepper-TB	0.941	1,10	158.95	0.004
Bean-TP	0.744	1,10	28.99	0.004
TP-TB	0.261	1,10	3.53	0.031

TP, coalescence of tomato and pepper microbiomes; TB, coalescence of tomato and bean microbiomes.

of health and fitness over a subsequent 3-month period. At weekly intervals over 5 weeks, flower counts increased and then plateaued around week 4, whereas fruit counts consistently increased (Figure S5C). In both cases during this period, microbiome treatment did not significantly impact the total numbers of these organs (Tables S3 and S4). At the end of the 3-month period, neither the cumulative production of fruit (Figure S5D; Table S5) nor total fruit weight (Figure S5E; Table S6) was significantly different among microbiome-treated plants or controls, but the plants treated with the tomato-bean coalescence microbiome had somewhat higher numbers of fruit (Tukey's HSD $p = 0.13$) and trended toward greater total fruit weight (Tukey's HSD $p = 0.07$) than plants treated with the heat-killed inoculum. The average weight of tomatoes did not differ by treatment or from the controls ($p > 0.05$, Figure S5F, Table S7). Finally, the total number of seeds from the oldest 3 ripe fruits of each plant did not significantly vary among treatments (Figure S5G; Table S8) nor did the proportion of seeds that could germinate (Figure S5H; Table S9). Thus, although experimental microbiomes differ in their ability to establish and flourish on a given plant species, we find little to no evidence for effects on host plant health or fitness.

Interrogation of the effects of host swapping in novel host environments

To determine how transmission history alters the outcome of microbiome assembly, we sprayed each host swapping line onto a set of novel plant hosts (canola, corn, and sorghum) and tomato and then compared with the tomato conspecific transmission lines sprayed onto the same set of host species (Figure 5A). Compositional variation among resultant microbiomes is explained by both recipient host species identity (PERMANOVA $R^2 = 0.181$, $p < 0.001$; Figure S3C) and microbiome history ($R^2 = 0.117$, $p < 0.001$), with an additional effect of experimental block ($R^2 = 0.080$, $p < 0.01$) but no significant interaction between these factors. When we substitute transmission mode (conspecific versus host swapping) for microbiome history, we also see an overall effect ($R^2 = 0.025$, $p < 0.05$). Pairwise PERMANOVA reveals that all host comparisons are significantly different in microbiome composition ($p_{adj} < 0.05$) and that all microbiome history comparisons are significantly different ($p_{adj} < 0.05$), with the exception of tomato conspecific lines and pepper host swap lines, which resulted in compositionally indistinguishable microbiomes ($p = 0.141$). The ASV-level taxonomic richness of the resultant microbiomes is significantly higher in the canola host plants ($p < 0.001$) than the tomato, corn, and sorghum hosts, which are indistinguishable from one another.

When we examine microbiome composition based on the transmission history of the inoculum, we see that all three groups from the host swapping lines resulted in microbiomes with weaker species identity effects than the conspecifically transmitted group (Figure 5B). In other words, the differences between the resultant canola, corn, sorghum, and tomato microbiomes were less pronounced when the inocula came from host swapping lines.

To examine the amount of bacterial microbiome multiplication on the host plants, we initially quantified the number of bacterial cells in each inoculum and subsequently measured the number of bacterial cells in the resultant microbiomes 1 week after their establishment on the plant hosts in the greenhouse. Inocula contained 2.2×10^5 to 4.6×10^7 total bacterial cells, and the subsequent microbiomes grew to 6.6×10^5 to 1.7×10^8 total bacterial cells (1.7×10^4 to 1.6×10^7 bacterial cells per g plant material), an average increase of 19.9-fold. All control plants receiving a sterile inoculum developed significantly lower bacterial abundances than individuals receiving a live inoculum ($p < 0.001$). We find that bacterial abundance per gram of plant material is shaped mostly by not only host species identity ($F_{3, 71} = 80.9$, $p < 0.001$) but also microbiome history ($F_{3, 71} = 2.79$, $p < 0.05$; Figure 5C). Post hoc analysis reveals that canola plants harbor the least abundant bacterial communities ($p < 0.001$), whereas corn and sorghum harbor the highest ($p < 0.001$). Similar qualitative conclusions regarding host effects of bacterial abundance were reached through culturing of cells in leaf washings ($F_{3, 71} = 24.6$, $p < 0.001$), except that no microbiome history effect is detected ($p = 0.871$), and instead, a host-by-microbiome history interaction is observed ($F_{9, 67} = 2.1$, $p < 0.05$). The range of microbiome growth factor (i.e., fold growth) is 0.07–322.8 and is influenced by host plant species identity ($F_{3, 69} = 3.4$, $p < 0.05$), with canola hosts harboring the lowest fold increase and corn and sorghum harboring the highest (Figure 5D).

The taxa from the initial passaging experiment that were identified as enriched in the host swapping lines not only persist in the microbiomes of these novel hosts but also collectively comprise a majority of the sequencing reads on these plants (79.4% ± 0.15%). When we transform these relative abundances by the droplet digital PCR (ddPCR)-inferred absolute abundance estimates of each of the microbiomes, we see that the host swap enriched taxa collectively grew to a range of 6.9×10^3 to 1.5×10^7 (median = 9.0×10^5) cells per g plant material.

Finally, to examine the resilience, or fidelity, of microbiome transplantation, we calculated the Bray-Curtis dissimilarity of the resultant microbiomes on these novel host plants to the samples from which the inocula were derived. This level of divergence was significantly shaped both by the host species identity of the recipient plant ($F_{3, 89} = 8.21$, $p < 0.001$) and the history of the microbiome being inoculated ($F_{3, 89} = 4.14$, $p < 0.01$). When we

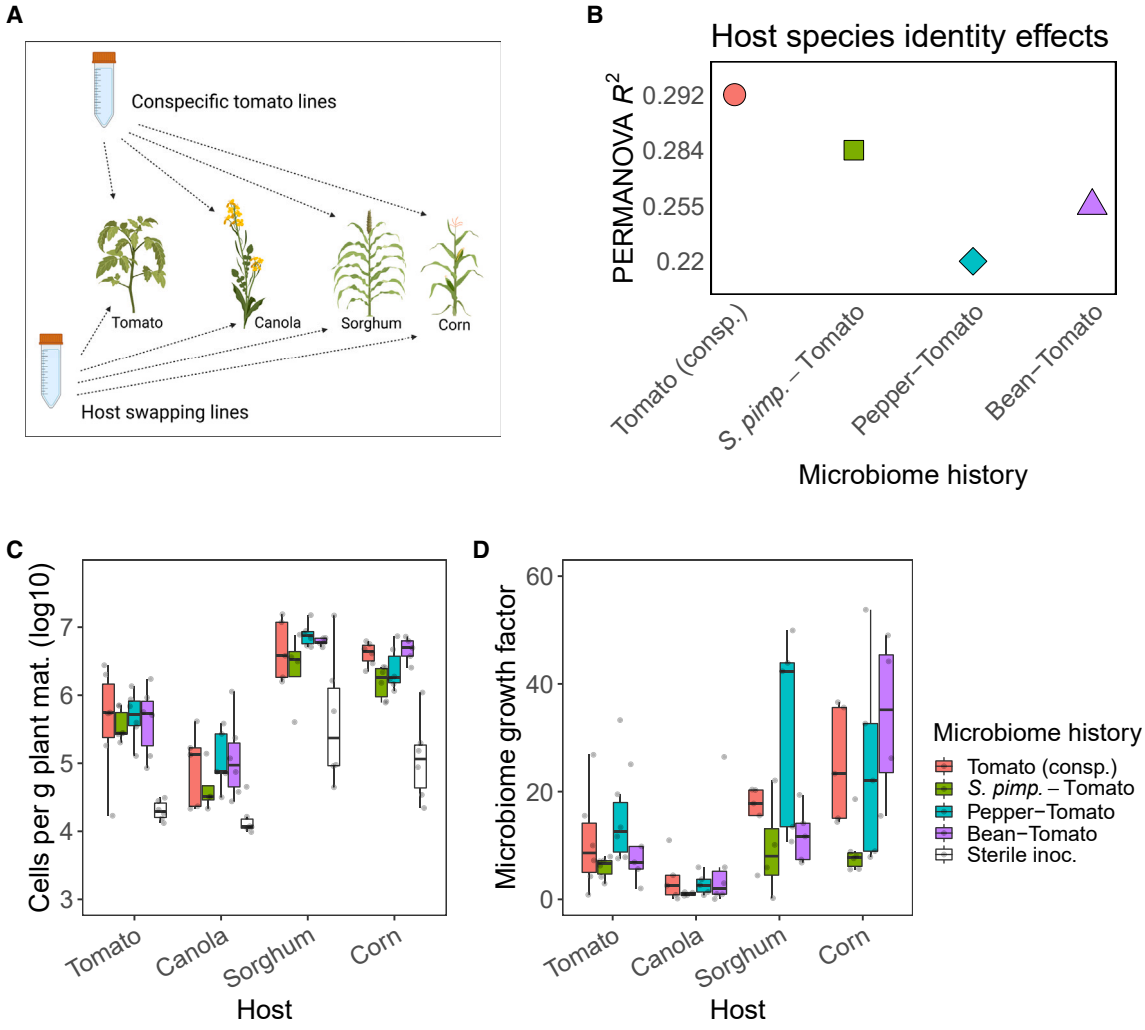

Figure 5. Transplantation of bacterial microbiomes onto novel plant hosts reveals effects of transmission mode, microbiome history, and recipient plant species identity

(A) Experimental design schematic illustrating the bacterial microbiome treatment inoculations onto novel host species. Experimental plant species include canola, sorghum, corn, and tomato, and microbiome treatments include conspecifically passaged tomato microbiomes as well as *S. pimpinellifolium*—tomato, pepper-tomato, and bean-tomato host swapping lines. Each treatment/plant combination has 6 replicate plants, and each plant species has 6 replicate sterile inoculum controls.

(B) Host species identity effects (PERMANOVA R^2 values, y axis), representing the distinction among microbiomes by host plant species identity, are lower in the microbiome lines (x axis) with a history of host swapping.

(C) Bacterial cells per g leaf material ($\log_{10}$ scale, y axis) is shaped by host species identity (x axis) and microbiome history (box color).

(D) Bacterial microbiome growth rate (y axis) as calculated from the estimated total cells inoculated onto leaf surface divided by the estimated total cells recovered from the leaves 1 week later. Data are separated by host species identity (x axis) and colored by microbiome history. For C and D, the bottom and top edges of boxes represent the 25th and 75th percentile, respectively, and lines in the box represent median values. Box whiskers represent data, excluding outliers, that fell more than 1.5 times the interquartile range below the first or above the third quartile.

substitute transmission mode for microbiome history, we also see a significant effect on divergence ($F_{1,\ 91} = 3.95$, $p < 0.05$) in which conspecifically passaged microbiomes diverge more than that of host swapping microbiomes. Post hoc analysis reveals that the communities assembled from conspecifically passaged tomato lines diverged more from their inoculum than the host-swapped *S. pimpinellifolium* lines (Tukey HSD $p = 0.02$), with no other significant comparisons. The difference among recipient hosts is driven by tomato and sorghum plants harboring less divergent microbiomes than corn (Tukey HSD $p < 0.001$ and $p = 0.03$, respectively). We find no evidence for a host-by-microbiome history or a host-by-transmission mode interaction.

DISCUSSION

The early stages of microbiome assembly are dramatically shaped by dispersal,[33] particularly for microbiomes in relatively open habitats such as the phyllosphere. In the case of host-to-host transmission of microbiota, whether taxa arriving early in development come from related or unrelated hosts is likely to

be a critical determinant of not just individual microbiome function but perhaps also the (co)evolutionary trajectory of hosts and microbiomes over generations. Recent research has shown that neighboring vegetation can alter the course of phyllosphere microbiome assembly,[24] suggesting that the density and composition of the local plant community are likely key factors shaping adaptation of leaf-associated microbial taxa to their hosts. To better understand the consequences of bacterial transmission between members of the same host species (conspecifics) versus between members of different host species (heterospecifics) on bacterial microbiome structuring and/or specialization, we implemented a microbiome-passaging experiment where transmission mode was manipulated and then examined the consequences of these transmission modes during assembly on novel hosts and through experimental community coalescence. Our results suggest that the outcome of phyllosphere microbiome assembly depends on microbiome transmission history and that microbiomes transmitted among conspecific hosts develop a competitive edge during establishment, consistent with host specialization. We further demonstrate that microbiomes swapped among plant species at each passage become less impacted by plant filtering relative to those passaged consistently on the same host plant.

Use of successive passaging as a means to examine the effects of host filtering

Successive passaging is a promising way to examine how host filtering shapes the assembly, diversity, and stability of microbiomes. Host-filtering effects were clearly demonstrated throughout our study, indicating that different subsets of microbial taxa survive and reproduce on each of the plant host species (a result previously shown in a field setting[24]). Consistent with previous work,[34] we see a strong impact of passaging on microbiome composition (Table 1) alongside a roughly 2-fold reduction of ASV-level richness over the experiment (Figure 2A). This suggests that selective pressures, as imposed by the plant host and/or interactions within the microbiome, limit the establishment or persistence of many of the taxa from the diverse starting inoculum. Although all microbiome lines tended to converge on roughly similar richness levels, a trending difference could be observed between transmission modes ($p = 0.056$), with those passaged through heterospecific transmission harboring somewhat lower richness than their conspecific transmission counterparts. This may result from the compounding selective filters of both host plants. Evidence for host-imposed selection was also apparent when we examined phylogenetic clustering. Here, we found that the microbiomes on the solanaceous plants—tomato, *S. pimpinellifolium*, and pepper—were significantly phylogenetically clustered, suggesting that the traits under selection—by host filtering, as well as the experimental conditions—are phylogenetically conserved (Figure 2B). Interestingly, for bean-associated microbiomes, we see a trend away from phylogenetic clustering and toward overdispersion. This observation corroborates similar findings of overdispersion and high neutral model goodness-of-fit measures for bean phyllosphere microbiomes compared with tomato and pepper in the field.[24] Together, this suggests that beans may be more permissive hosts than tomato or pepper plants. In further support of this concept, host-swapped microbiomes involving bean plants trend in a similar phylogenetically overdispersed direction, suggesting a host-by-transmission mode interaction in selective pressures.

Further evidence of strong host filtering can be seen from the effects of microbiome history, i.e., patterns of microbiome differentiation structured by previous host association, observed in all three experiments. In the initial passaging experiment, each time the host swapping lines were transplanted onto tomato hosts, the resultant microbiomes remained statistically discernible in composition by their previous host association, suggesting that previous host filtering can impact subsequent assembly, likely by altering the species pool on which subsequent selection acts. Similarly, when microbiomes were transplanted onto novel hosts, microbiome history effects could be observed in the subsequent microbiome composition, diversity, and abundance (Figure 5C). Finally, when the conspecifically transmitted bean, pepper, and tomato microbiomes were transplanted onto tomato hosts in the specialization experiment, we saw a strong effect of microbiome history that resulted in distinguishable compositions and, in the case of microbiomes with a bean-association history, a lower microbiome density (Figure 4C). Together, these observations demonstrate that transmission mode has a pronounced impact on the process of host microbiome filtering, likely by altering the source pool of microbial propagules.

Microbiomes passaged heterospecifically exhibit homogenization and host generalism

Previous work with phyllosphere microbiome passaging on different genotypes of tomato found evidence for reduced host identity effects over the course of microbiome selection.[34] In contrast, we find that host identity effects at the species level are retained over time even as microbiome composition shifts in response to selection. Importantly, this was not true of our host swapping (heterospecific transmission) lines, suggesting that this form of transmission might homogenize microbiomes and/or select for more generalist taxa that resist host selective filters (Figure 3A). This pattern was further exemplified when we transplanted the resultant microbiomes onto a set of novel hosts. Here, the conspecifically passaged microbiomes were found to exhibit higher host species identity effects than each of the 3 host swapping lines (Figure 5B), suggesting that the host swap lines are less impacted by the selective filters of the various hosts. Moreover, our differential presence/absence models identified several taxa in the host swapping groups that were more likely to establish on these novel hosts relative to their conspecific transmission counterparts. These taxa collectively grew to high densities on the novel hosts and comprised a majority of the resultant microbiomes, suggesting that they may exhibit host generalism and thereby be less impacted by host filtering. Overall, our experimental results suggest that repeated heterospecific transmission has a homogenizing effect on microbiomes and may favor certain microbial taxa with high engraftability on novel hosts.

Transmission mode shapes microbiome network structure

In addition to differences in the effects of host filtering, another apparent difference in the host swapping versus conspecific transmission lines is in network structure. The co-occurrence networks constructed from the three independent host swapping microbiome lines consistently exhibited a higher clustering coefficient

than their conspecific transmission counterparts (Figure 3B), meaning that edges to a node (i.e., neighbors) tend to be more connected with each other. One implication of a higher clustering coefficient is that the networks could be more resilient to perturbation, such that the loss of any node would be less disruptive to the overall network due to the higher interconnectedness of edges.[35] This observation may shed light on the selective pressures the microbiomes face during heterospecific transmission. For instance, if the host swapping treatments face a broader set of host filters by transmitting across two host species, then the development of a more highly clustered network could provide additional stability. Interestingly, we see that the conspecific transmission lines consistently exhibit a higher number of network edges than their host swapping counterparts (Figure 3C). This may be afforded by the constancy of the host environment that the conspecific transmission lines face. Although the use of ecological networks to infer microbial interactions may be limited at relatively large spatial scales such as an entire plant or through relative abundance measurements,[36] the fact that we see these consistent trends across independent biological replicates provides support for the notion that network attributes are in part shaped by transmission mode. Nevertheless, additional fine-scale work to interrogate microbe-microbe interactions and microbiome resiliency resulting from transmission manipulation would undoubtedly reveal additional insights into patterns of microbial interactions.

Conspecific transmission facilitates host specialization: Evidence from experimental community coalescence

Community coalescence (i.e., mixing) has been proposed as a framework to examine community-level competition and functionality.[29,37,38] Here, theory predicts that as communities adapt to local conditions through individual member adaptation, cooperation among individual members, or emergence of higher order strategies, they may develop a local competitive edge and hence be more likely to displace competitively inferior communities.[39–41] We implemented this framework to examine whether microbiomes could become specialized, i.e., locally adapted, on a given host species through repeated conspecific transmission. We applied microbiomes with a history of tomato, pepper, and bean conspecific transmission to tomato hosts either by themselves or in 1:1 coalescence (competition) treatments and showed that in both coalescence treatments, the resultant microbiomes became dominated by the tomato-associated microbiome (Figure 4C; Table 2). Interestingly, the degree to which the coalescence treatments became dominated by tomato microbiomes exhibited a host phylogenetic trend consistent with phylosymbiosis theory[42]; with the microbiomes from bean—a much more distantly related host—becoming more dominated than the microbiomes from pepper—a member of the same family as tomato (Solanaceae). Thus, due to the prior repeated assembly history of the tomato-associated microbiomes, these microbiomes exhibited a "home field advantage" on tomato hosts over the pepper- and bean-associated microbiomes, resulting in competitive dominance. These results could be relevant to the conservation of species that are becoming increasingly rare[32] and thus less likely to receive specialized microbial propagules. Our results may also be relevant to microbiome engineering efforts, where vigorous establishment and resistance to invasion are desired microbiome characteristics.[27]

Despite the compositional differences among the experimental microbiome treatments in the specialization experiment and the degree to which the microbiomes exhibited host specialization, we found no evidence to suggest that such microbiome differences impacted host health, fitness, or leaf transcriptional activity. Intriguingly, under germfree conditions, *Arabidopsis thaliana* has been shown to exhibit some distinct transcriptional responses to individual strains of bacteria when applied as monoassociations.[43] Although we used a different plant species for our study, our data contribute to this narrative by suggesting that such strain-level differences in host transcription may disappear when leaf microbiomes are of a higher complexity or when plants have not been maintained under strict axenic conditions. Although the presence of a phyllosphere microbiome has been shown to have substantial impacts on host traits such as disease resistance and growth, making it a focus of microbiome engineering efforts,[27,44] the compositional differences of that microbiome apparently have a far lesser effect on the plant transcriptome. Taken together, these data suggest that microbiome-level specialization to plant hosts does not necessarily imply effects on the health, fitness, or transcriptional activity of the host.

Concluding remarks: Better understanding of the role of transmission in shaping microbiome assembly and function

Transmission mode has long been recognized as a key factor shaping the life history strategies of pathogens and other symbionts. Whether such a paradigm applies to complex assemblages of microorganisms residing in or on hosts has remained relatively overlooked. With increasing recognition of the role microbiomes play in plant health, agriculture, and resilience to climate change, it is imperative that we better understand the processes of microbiome assembly and host specialization. Although much of the focus of the plant microbiome literature has been on the role the plant host plays in microbiome selection, our results show that by limiting the microbial species pool from which assembly can take place, transmission mode alters the outcome of assembly. We show that conspecific transmission can confer a competitive advantage whereby microbiomes outcompete invading microbiomes with a different host association history and that host swapping may homogenize microbiomes but confer a broader host range upon them. Such results shed light on how patterns of host-microbiome co-diversification (and phylosymbiosis) may emerge as a result of consistent associations over evolutionary time. Future work could examine whether these patterns are consistent for other groups inhabiting the phyllosphere, e.g., fungi or protists, and work toward identifying the underlying molecular mechanisms by which microbial taxa within microbiomes respond and adapt to their specific host environment. Finally, these results serve as a promising demonstration that by altering transmission mode, microbiome engineering efforts can be directed toward host fidelity and invasion resistance or toward broad-range host generalism with taxa refractory to host filtering.

STAR★METHODS

Detailed methods are provided in the online version of this paper and include the following:

SUPPLEMENTAL INFORMATION

Supplemental information can be found online at https://doi.org/10.1016/j.chom.2023.11.002.

ACKNOWLEDGMENTS

We thank Adam McCurdy and the other farming staff at Coastal Roots Farm in Encinitas, CA and the UC-Davis student farm for providing access to tomato leaves to serve as initial inoculum. We thank R. Porch for assistance in collecting leaves for the initial inoculum. We thank C. Wistrom and the Oxford greenhouse staff at UC Berkeley for their support throughout the experiment. We thank J. Tomorsky for guidance and helpful advice pertaining to RNA-seq bioinformatics. Figures 1, 4A, and 5A were created with BioRender.com. This study was funded by the US National Science Foundation, award no. 1754494. B.K. is a Chan Zuckerberg Biohub–San Francisco investigator.

AUTHOR CONTRIBUTIONS

K.M.M., S.E.L., C.J.E.M., and B.K. conceptualized and designed the experiments. K.M.M., A.L.S.V., J.K.S., and I.E.M. performed the experiments and processed the samples. K.M.M. performed data processing, analysis, and writing of the initial draft. All authors contributed to the writing and editing of the paper.

DECLARATION OF INTERESTS

The authors declare no competing interests.

Received: June 26, 2023
Revised: September 9, 2023
Accepted: November 1, 2023
Published: November 28, 2023

REFERENCES

1. Leftwich, P.T., Edgington, M.P., and Chapman, T. (2020). Transmission efficiency drives host–microbe associations. Proc. Biol. Sci. *287*, 20200820.
2. Moeller, A.H., Suzuki, T.A., Phifer-Rixey, M., and Nachman, M.W. (2018). Transmission modes of the mammalian gut microbiota. Science *362*, 453–457.
3. Fisher, R.M., Henry, L.M., Cornwallis, C.K., Kiers, E.T., and West, S.A. (2017). The evolution of host-symbiont dependence. Nat. Commun. *8*, 15973.
4. Stewart, A.D., Logsdon, J.M., and Kelley, S.E. (2005). An empirical study of the evolution of virulence under both horizontal and vertical transmission. Evolution *59*, 730–739.
5. Frank, S.A. (1996). Models of parasite virulence. Q. Rev. Biol. *71*, 37–78.
6. Ehinger, M., Mohr, T.J., Starcevich, J.B., Sachs, J.L., Porter, S.S., and Simms, E.L. (2014). Specialization-generalization trade-off in a Bradyrhizobium symbiosis with wild legume hosts. BMC Ecol. *14*, 8.
7. Ebert, D. (1994). Virulence and local adaptation of a horizontally transmitted parasite. Science *265*, 7–9.
8. Chomicki, G., Kiers, E.T., and Renner, S.S. (2020). The evolution of mutualistic dependence. Annu. Rev. Ecol. Evol. Syst. *51*, 409–432.
9. Lindow, S.E., and Brandl, M.T. (2003). Microbiology of the phyllosphere. Appl. Environ. Microbiol. *69*, 1875–1883.
10. Koskella, B. (2020). The phyllosphere. Curr. Biol. *30*, R1143–R1146.
11. Morella, N.M., Zhang, X., and Koskella, B. (2019). Tomato seed-associated bacteria confer protection of seedlings against foliar disease caused by Pseudomonas syringae. Phytobiomes J. *3*, 177–190.
12. Innerebner, G., Knief, C., and Vorholt, J.A. (2011). Protection of Arabidopsis thaliana against leaf-pathogenic Pseudomonas syringae by Sphingomonas strains in a controlled model system. Appl. Environ. Microbiol. *77*, 3202–3210.
13. Berg, M., and Koskella, B. (2018). Nutrient- and dose-dependent microbiome-mediated protection against a plant pathogen. Curr. Biol. *28*, 2487–2492.e3.
14. Spaepen, S., and Vanderleyden, J. (2011). Auxin and plant-microbe interactions. Cold Spring Harb. Perspect. Biol. *3*, a001438.
15. Laforest-Lapointe, I., Paquette, A., Messier, C., and Kembel, S.W. (2017). Leaf bacterial diversity mediates plant diversity and ecosystem function relationships. Nature *546*, 145–147.
16. Vorholt, J.A. (2012). Microbial life in the phyllosphere. Nat. Rev. Microbiol. *10*, 828–840.
17. Ottesen, A.R., Gorham, S., Reed, E., Newell, M.J., Ramachandran, P., Canida, T., Allard, M., Evans, P., Brown, E., and White, J.R. (2016). Using a control to better understand phyllosphere microbiota. PLoS One *11*, e0163482.
18. Yadav, R.K.P., Karamanoli, K., and Vokou, D. (2005). Bacterial colonization of the phyllosphere of Mediterranean perennial species as influenced by leaf structural and chemical features. Microb. Ecol. *50*, 185–196.
19. Hacquard, S., Spaepen, S., Garrido-Oter, R., and Schulze-Lefert, P. (2017). Interplay between innate immunity and the plant microbiota. Annu. Rev. Phytopathol. *55*, 565–589.
20. Jones, J.D.G., and Dangl, J.L. (2006). The plant immune system. Nature *444*, 323–329.
21. Bodenhausen, N., Bortfeld-miller, M., Ackermann, M., and Vorholt, J.A. (2014). A synthetic community approach reveals plant genotypes affecting the phyllosphere microbiota. PLoS Biol. *10*, e1004283.
22. Custer, G.F., Bresciani, L., and Dini-Andreote, F. (2022). Ecological and evolutionary implications of microbial dispersal. Front. Microbiol. *13*, 855859.
23. Lindow, S.E., and Andersen, G.L. (1996). Influence of immigration on epiphytic bacterial populations on navel orange leaves. Appl. Environ. Microbiol. *62*, 2978–2987.
24. Meyer, K.M., Porch, R., Muscettola, I.E., Vasconcelos, A.L.S., Sherman, J.K., Metcalf, C.J.E., Lindow, S.E., and Koskella, B. (2022). Plant neighborhood shapes diversity and reduces interspecific variation of the phyllosphere microbiome. ISME J. *16*, 1376–1387.
25. Lajoie, G., and Kembel, S.W. (2021). Host neighborhood shapes bacterial community assembly and specialization on tree species across a latitudinal gradient. Ecol. Monogr. *91*, 1–18.
26. Laforest-Lapointe, I., Messier, C., and Kembel, S.W. (2016). Host species identity, site and time drive temperate tree phyllosphere bacterial community structure. Microbiome *4*, 27.

27. Zhan, C., Matsumoto, H., Liu, Y., and Wang, M. (2022). Pathways to engineering the phyllosphere microbiome for sustainable crop production. Nat. Food *3*, 997–1004.

28. Batstone, R.T., O'Brien, A.M., Harrison, T.L., and Frederickson, M.E. (2020). Experimental evolution makes microbes more cooperative with their local host genotype. Science *370*, 23–26.

29. Rocca, J.D., Muscarella, M.E., Peralta, A.L., Izabel-Shen, D., Simonin, M., Shade, A., and Diaz-Colunga, J. (2021). Guided by microbes: applying community coalescence principles for predictive microbiome engineering. mSystems *0*. e00538–00521.

30. Chang, C.-Y., Vila, J.C.C., Bender, M., Li, R., Mankowski, M.C., Bassette, M., Borden, J., Golfier, S., Sanchez, P.G.L., Waymack, R., et al. (2021). Engineering complex communities by directed evolution. Nat. Ecol. Evol. *5*, 1011–1023.

31. Busby, P.E., Soman, C., Wagner, M.R., Friesen, M.L., Kremer, J., Bennett, A., Morsy, M., Eisen, J.A., Leach, J.E., and Dangl, J.L. (2017). Research priorities for harnessing plant microbiomes in sustainable agriculture. PLoS Biol. *15*, e2001793.

32. Trevelline, B.K., Fontaine, S.S., Hartup, B.K., and Kohl, K.D. (2019). Conservation biology needs a microbial renaissance: a call for the consideration of host-associated microbiota in wildlife management practices. Proc. Biol. Sci. *286*, 20182448.

33. Zhou, J., and Ning, D. (2017). Stochastic community assembly: does it matter in microbial ecology? Microbiol. Mol. Biol. Rev. *81*, e00002–e00017.

34. Morella, N.M., Weng, F.C.H., Joubert, P.M., Metcalf, C.J.E., Lindow, S., and Koskella, B. (2020). Successive passaging of a plant-associated microbiome reveals robust habitat and host genotype-dependent selection. Proc. Natl. Acad. Sci. USA *117*, 1148–1159.

35. Minor, E.S., and Urban, D.L. (2008). A graph-theory framework for evaluating landscape connectivity and conservation planning. Conserv. Biol. *22*, 297–307.

36. Blanchet, F.G., Cazelles, K., and Gravel, D. (2020). Co-occurrence is not evidence of ecological interactions. Ecol. Lett. *23*, 1050–1063.

37. Rillig, M.C., Antonovics, J., Caruso, T., Lehmann, A., Powell, J.R., Veresoglou, S.D., and Verbruggen, E. (2015). Interchange of entire communities: microbial community coalescence. Trends Ecol. Evol. *30*, 470–476.

38. Sierocinski, P., Milferstedt, K., Bayer, F., Großkopf, T., Alston, M., Bastkowski, S., Swarbreck, D., Hobbs, P.J., Soyer, O.S., Hamelin, J., et al. (2017). A single community dominates structure and function of a mixture of multiple methanogenic Communities. Curr. Biol. *27*, 3390–3395.e4.

39. Gilpin, M. (1994). Community-level competition: asymmetrical dominance. Proc. Natl. Acad. Sci. USA *91*, 3252–3254.

40. Toquenaga, Y. (1997). Historicity of a simple Competition Model. J. Theor. Biol. *187*, 175–181.

41. Sánchez, Á., Vila, J.C.C., Chang, C.Y., Diaz-Colunga, J., Estrela, S., and Rebolleda-Gomez, M. (2021). Directed evolution of microbial communities. Annu. Rev. Biophys. *50*, 323–341.

42. Brooks, A.W., Kohl, K.D., Brucker, R.M., Van Opstal, E.J., and Bordenstein, R. (2016). Phylosymbiosis: relationships and functional effects of microbial communities across host evolutionary history. PLoS Biol. *14*, 1–29.

43. Vogel, C., Bodenhausen, N., Gruissem, W., and Vorholt, J.A. (2016). The Arabidopsis leaf transcriptome reveals distinct but also overlapping responses to colonization by phyllosphere commensals and pathogen infection with impact on plant health. New Phytol. *212*, 192–207.

44. Stone, B.W.G., Weingarten, E.A., and Jackson, C.R. (2018). The role of the phyllosphere microbiome in plant health and function. In Annual Plant Reviews Online (Wiley), pp. 533–556.

45. Carini, P., Marsden, P.J., Leff, J.W., Morgan, E.E., Strickland, M.S., and Fierer, N. (2016). Relic DNA is abundant in soil and obscures estimates of soil microbial diversity. Nat. Microbiol. *2*, 16242.

46. Chelius, M.K., and Triplett, E.W. (2001). The diversity of Archaea and bacteria in association with the roots of Zea mays L. Microb. Ecol. *41*, 252–263.

47. Bodenhausen, N., Horton, M.W., and Bergelson, J. (2013). Bacterial communities associated with the leaves and the roots of Arabidopsis thaliana. PLoS One *8*, e56329.

48. Lundberg, D.S., Yourstone, S., Mieczkowski, P., Jones, C.D., and Dangl, J.L. (2013). Practical innovations for high-throughput amplicon sequencing. Nat. Methods *10*, 999–1002.

49. Callahan, B.J., McMurdie, P.J., Rosen, M.J., Han, A.W., Johnson, A.J.A., and Holmes, S.P. (2016). DADA2: high-resolution sample inference from Illumina amplicon data. Nat. Methods *13*, 581–583.

50. R Core Team (2020). R: A Language and Environment for Statistical Computing (R Foundation for Statistical Computing).

51. Morgan, M., Anders, S., Lawrence, M., Aboyoun, P., Pagès, H., and Gentleman, R. (2009). ShortRead: a bioconductor package for input, quality assessment and exploration of high-throughput sequence data. Bioinformatics *25*, 2607–2608.

52. Pagès, H., Aboyoun, P., Gentleman, R., and DebRoy, S. (2020). Biostrings: efficient manipulation of biological strings. https://rdrr.io/bioc/Biostrings/.

53. McMurdie, P.J., and Holmes, S. (2013). phyloseq: an R package for reproducible interactive analysis and graphics of microbiome census data. PLoS One *8*, e61217.

54. Wang, Q., Garrity, G.M., Tiedje, J.M., and Cole, J.R. (2007). Naive bayesian classifier for rapid assignment of rRNA sequences into the new bacterial taxonomy. Appl. Environ. Microbiol. *73*, 5261–5267.

55. Quast, C., Pruesse, E., Yilmaz, P., Gerken, J., Schweer, T., Yarza, P., Peplies, J., and Glöckner, F.O. (2013). The SILVA ribosomal RNA gene database project: improved data processing and web-based tools. Nucleic Acids Res. *41*, D590–D596.

56. Davis, N.M., Proctor, D.M., Holmes, S.P., Relman, D.A., and Callahan, B.J. (2018). Simple statistical identification and removal of contaminant sequences in marker-gene and metagenomics data. Microbiome *6*, 226.

57. Andrews, S. (2010). FASTQC. A quality control tool for high throughput sequence data. https://www.bioinformatics.babraham.ac.uk/projects/fastqc/.

58. Alonge, M., Soyk, S., Ramakrishnan, S., Wang, X., Goodwin, S., Sedlazeck, F.J., Lippman, Z.B., and Schatz, M.C. (2019). RaGOO: fast and accurate reference-guided scaffolding of draft genomes. Genome Biol. *20*, 224.

59. Fernandez-Pozo, N., Menda, N., Edwards, J.D., Saha, S., Tecle, I.Y., Strickler, S.R., Bombarely, A., Fisher-York, T., Pujar, A., Foerster, H., et al. (2015). The Sol Genomics Network (SGN)–from genotype to phenotype to breeding. Nucleic Acids Res. *43*, D1036–D1041.

60. Dobin, A., Davis, C.A., Schlesinger, F., Drenkow, J., Zaleski, C., Jha, S., Batut, P., Chaisson, M., and Gingeras, T.R. (2013). STAR: ultrafast universal RNA-seq aligner. Bioinformatics *29*, 15–21.

61. Oksanen, J., Blanchet, F.G., Roeland, K., Legendre, P., Minchin, P., O'Hara, R.B., Simpson, G., Solymos, P., Stevens, M.H.H., and Wagner, H. (2015). Vegan: community ecology package. R Package Version 2.2-0. http://CRAN.Rproject.org/package=vegan.

62. Anderson, M.J. (2001). A new method for non-parametric multivariate analysis of variance. Austral Ecol. *26*, 32–46.

63. Wright, E.S. (2016). Using DECIPHER v2.0 to analyze big biological sequence data in R. R J. *8*, 352–359.

64. Schliep, K.P. (2011). phangorn: phylogenetic analysis in R. Bioinformatics *27*, 592–593.

65. Kembel, S.W., Cowan, P.D., Helmus, M.R., Cornwell, W.K., Morlon, H., Ackerly, D.D., Blomberg, S.P., and Webb, C.O. (2010). Picante: R tools for integrating phylogenies and ecology. Bioinformatics *26*, 1463–1464.

66. Harrell, F.E. (2020). Hmisc: Harrell Miscellaneous. hbiostat.org/r/hmisc.

CellPress
OPEN ACCESS

67. Csárdi, G., and Nepusz, T. (2006). The Igraph software package for complex network research. InterJournal Complex Syst. *1695*, 1–9.

68. Debray, R., Socolar, Y., Kaulbach, G., Guzman, A., Hernandez, C.A., Curley, R., Dhond, A., Bowles, T., and Koskella, B. (2022). Water stress and disruption of mycorrhizas induce parallel shifts in phyllosphere microbiome composition. New Phytol. *234*, 2018–2031.

69. Kuznetsova, A., Brockhoff, P.B., and Christensen, R.H.B. (2017). lmerTest package: tests in linear mixed effects models. J. Stat. Softw. *82*, 1–26.

70. Bürkner, P.-C. (2017). brms: an R package for Bayesian Multilevel Models Using Stan. J. Stat. Softw. *80*, 1–28.

71. Robinson, M.D., Mccarthy, D.J., and Smyth, G.K. (2010). edgeR: a Bioconductor package for differential expression analysis of digital gene expression data. Bioinformatics *26*, 139–140.

STAR★METHODS

KEY RESOURCES TABLE

REAGENT or RESOURCE	SOURCE	IDENTIFIER
Chemicals, peptides, and recombinant proteins		
$MgCl_2$	Sigma Aldrich	Cat: 7786-30-3
Sodium hypochlorite (7% available chlorine)	Sigma Aldrich	Cat: 13440
PMA	Sigma Aldrich	Cat: 16561-29-8
Critical commercial assays		
DNeasy PowerSoil kit	Qiagen	Cat: 47014
Spectrum Plant Total RNA Kit	Merck/MilliporeSigma, MO, USA	Cat: STRN50
BIO-RAD QX 200 Droplet Reader	Bio-Rad Laboratories, Hercules, CA, USA	Cat: 1864003
Deposited data		
BioProject	PRJNA1012508	N/A
Figshare		https://doi.org/10.6084/m9.figshare.22280884
Experimental models: Organisms/strains		
Solanum lycopersicum var. Moneymaker	Parkseed, SC, USA	Cat #: 05851-PK-P1
Solanum pimpinellifolium	Seed savers exchange, IA, USA	Cat #: 1230A 1M
Capsicum annuum var. Early Cal Wonder	Parkseed, SC, USA	Cat #: 05844-PK-P1
Phaseolus vulgaris var. Bush Blue Lake 274	Parkseed, SC, USA	Cat #: 05010-PK-P1
Brassica napus subsp. *napus*	Annie's Heirloom Seeds, WI, USA	N/A
Sorghum bicolor var. BTx642	Peggy Lemaux, UC Berkeley	N/A
Zea mays convar. *saccharata* var. *rugosa*	Isla's Garden Seeds Company, ID, USA	Cat #: 100250
Oligonucleotides		
16S V5 sequencing 799F (5' – AACMGGAT TAGATACCCKG – 3')	N/A	N/A
16S V7 sequencing 1193R (5' – ACGTCA TCCCCACCTTCC – 3')	N/A	N/A
Software and algorithms		
DADA2 1.16	DADA2	https://benjjneb.github.io/dada2/index.html
Vegan 2.6-4	Vegan	https://cran.r-project.org/web/packages/vegan/index.html
STAR 2.7.11a	STAR	https://github.com/alexdobin/STAR
edgeR 3.17	edgeR	https://bioconductor.org/packages/release/bioc/html/edgeR.html
Picante 1.8.2	Picante	https://cran.r-project.org/web/packages/picante/index.html

RESOURCE AVAILABILITY

Lead contact

Further information and requests for resources or reagents should be directed to and will be fulfilled by the lead contact, Dr. Kyle Matthew Meyer (kmmeyer@berkeley.edu).

Materials availability

This study did not generate new reagents or materials.

Data and code availability

- 16S rRNA gene amplicon sequence data and RNAseq data have been deposited at the NCBI BioProject database (BioProject ID: PRJNA1012508).

CellPress
OPEN ACCESS

- Amplicon sequence data, metadata, microbiome phylogenetic tree, plant health and fitness data, and reproducible R code pertaining to this study are publicly available on figshare (https://doi.org/10.6084/m9.figshare.22280884).
- Any additional information required to reanalyze the data in this paper is available from the lead contact upon request.

Raw sequence data can be accessed at the NCBI BioProject database (BioProject ID: PRJNA1012508). Sequence data, metadata, and reproducible R code pertaining to this study are publicly available on figshare https://doi.org/10.6084/m9.figshare.22280884).

METHOD DETAILS

Experimental design - Passaging experiment

To generate the initial community for selection, we created a diverse microbial inoculum by sampling epiphytic (leaf surface) microbiomes from tomato leaves collected in two regions of California at separate times. The first collection was at Coastal Roots Farm, located in Encinitas, CA in May 2019, where plants were in early vegetative growth (pre-flowering) and had been established in the field for roughly 4 weeks. The second collection was at the University of California - Davis student organic farm in August 2019, where plants were 3-4 months old and in the fruit ripening stage. In both cases, leaves were excised from the plants, placed into sealable sterile 1-gallon plastic bags (Ziplock, USA), and transported in a chilled cooler to the laboratory and held at 4° C. The day following collection, epiphytic microbial members of the phyllosphere were gently dissociated from leaf surfaces using a sonicating water bath (Branson 5800) using a ratio of roughly 0.6 g of leaf material to 1 ml 10 mM $MgCl_2$. In total, 4.7 kg of leaf material were processed from the Encinitas collection and 2.4 kg from the Davis collection. Leaf wash was pelleted by centrifuging at 4000 rcf and 10° C for 10 minutes and then resuspended in KB broth and mixed in equal parts with 1:1 KB:glycerol for preservation at -20° C. The leaf wash from both collections was combined to serve as the initial inoculum for the experiment. Prior to combining, aliquots of each collection were set aside to later test whether they differed in establishment ability.

We used four plant hosts for passaging: cultivated tomato (*Solanum lycopersicum var.* Moneymaker), *Solanum pimpinellifolium* (tomato wild ancestor), bell pepper (*Capsicum annuum var.* Early Cal Wonder), and bush bean (*Phaseolus vulgaris* var. Bush Blue Lake 274). Due to differences in germination and development rate, seed planting times were adjusted so that plants were roughly equivalent in size at initial inoculation. Tomato and *S. pimpinellifolium* were 4.5 weeks post seed planting, peppers were 5.5 weeks, and beans were 2.5 weeks. All experimental plants were grown in Sunshine Mix 4 potting soil (Sungro Horticulture, USA) in a climate-controlled greenhouse with 12 hours of supplemental lighting without fertilizer or pesticide application at the University of California Berkeley Oxford Facility.

To begin the passaging experiment, 6 plants from each of the four hosts were inoculated with the same initial inoculum (Figures 1A and 1B), which was prepared by thawing the freezer stock, centrifuging at 4000 rcf and 10° C for 10 minutes to pellet cells, decanting the supernatant, and re-suspending cells in sterile 10 mM $MgCl_2$. For the first week of inoculation, inoculum volumes per plant were 4 ml for tomato, *S. pimpinellofolium*, and bean plants, and 3 ml for the slightly smaller pepper plants. Inocula were sprayed onto the adaxial (top) and abaxial (bottom) sides of leaves using ethanol- and UV-sterilized hand-held misters. After inoculation, the moist, sprayed plants were placed in a chamber maintaining ca. 100% relative humidity for 20 hours in order to maintain leaf moistness, thus encouraging microbial growth, before being transferred to a greenhouse. In both cases, plant location on the bench was randomized among treatments. Because of both space limitations in the misting chamber, and the scale of inoculations, we divided the plants into 2 blocks, such that block 1 contained replicates 1–3 and the blank (no inoculum) controls, all of which were sprayed on one day, while block 2 contained replicates 4–6, all of which were sprayed 2 days later. Plants from experimental blocks 1 and 2 were placed on different adjacent benches. A week later plants received a second inoculation following the same procedure, but with slightly higher inoculum volumes: 5 ml per plant for tomato, *S. pimpinellifolium*, and bean plants and 3.5 ml for pepper plants. The plants were then returned to the greenhouse for another week. 1 week after the final inoculation (2 weeks since the first inoculation), leaf material from each plant was excised using ethanol-sterilized scissors, placed in separate sterile plastic bags (Ziplock, USA), and transported in a chilled cooler to the laboratory where it was then weighed and combined with 200 mL sterile 10 mM $MgCl_2$ and sonicated as described above. Cells from each microbiome sample were then pelleted and preserved using the above-described centrifugation procedure.

During each subsequent passage, experimental plants were inoculated once per week for 3 weeks, followed by a week in the greenhouse. Independent microbiome lines were maintained for every experimental replicate. Inocula were prepared at the end of each passage in the same way as described above for the initial inoculation. The inoculum volume applied increased successively from week 1 to 3 to account for plant growth. The experiment involved 2 treatment types: 1) conspecific transmission, whereby 6 replicate community lines were passaged between members of the same plant species for 6 successive passages (Figure 1A), and 2) heterospecific transmission (i.e. host swapping), whereby 6 replicate lines of communities started on non-tomato plants (i.e *S. pimpinellifolium*, pepper, and bean) were inoculated onto tomato plants every other passage (i.e. for passages 2, 4, and 6), thus disrupting conspecific transmission (Figure 1B). The two experimental controls were: 1) blank inoculum, wherein sterile 10 mM $MgCl_2$ was sprayed onto 1 plant of each species at each passage in order to survey the diversity and identity of microbes that might establish in the greenhouse environment, and 2) a seasonality control, in which an aliquot of the combined initial inoculum was sprayed onto 3 replicate tomato plants in order to ask whether similar initial selection results were obtained at each passage throughout the experiment. Thus, from passage 2 to 6, each passage involved 49 plants, 24 of which were conspecific transmission lines (6 tomato, 6 *S. pimpinellifolium*, 6 pepper, and 6 bean), 18 of which were heterospecific lines (*S. pimpinellifolium*-tomato,

pepper-tomato, and bean-tomato), and 7 were controls (4 blank and 3 seasonality). Since the seasonality controls did not start until passage 2, Passage 1 had 46 plants, bringing the total number of samples to 291 plants. The six experimental passages took place between September 2019 and July 2020, with every plant of each replicate lineage surviving.

Microbiome specialization experiment after final passage using experimental community coalescence

To test for microbiome host specialization, we devised a community coalescence experiment involving the microbiome lines that were conspecifically passaged on tomato, pepper, or bean hosts. For each plant species, the six replicate lines were combined into a single inoculum. The live bacterial cells in each of these 3 groups were quantified using PMA treatment followed by droplet digital PCR (ddPCR) targeting cells with 16S rRNA gene copies.[34,45] Each week for 3 weeks these groups were combined, quantified, and adjusted to the lowest concentration needed to equalize live bacterial cell numbers. Equalized live cell totals were 1.82×10^5, 1.38×10^5, and 1.44×10^5 cells for weeks 1, 2, and 3, respectively. Coalescence treatments were devised by combining the tomato and pepper groups and the tomato and bean groups at a 1:1 ratio of live cells. Following equalization, each group was split into 6 tubes and adjusted to 3.5 ml total volume using sterile 10 mM $MgCl_2$ to serve as replicate inocula at roughly 8.6×10^3, 6.6×10^3, and 6.9×10^3 live cells per ml concentration, respectively. All inocula were sprayed onto the abaxial and adaxial side of 5-week-old moneymaker tomato leaves following the same procedure as the main passaging experiment. Two experimental controls were included: 6 replicate blank inoculum controls, in which sterile 10 mM $MgCl_2$ was applied at the same volume as the treatment plants, and 6 replicate heat-killed controls, in which inocula containing the same concentration of live cells as the treatment plants were autoclaved for 40 minutes to kill the cells. Thus, the total treatments were microbiomes from P6 conspecific tomato lines (n=6), P6 conspecific pepper lines (n=6), P6 conspecific bean lines (n=6), coalescence of P6 tomato and pepper (n=6), coalescence of P6 tomato and bean (n=6), blank inoculum controls (n=6), and heat-killed inoculum controls (n=6), with a total of 42 plants. After 3 sequential inoculations and a 1-week incubation period, roughly 1/3 of the leaves (leaf weight range 12.1 – 33.4 g, median = 21.4 g) from the 42 experimental plants were harvested and processed using the same leaf wash protocol as the passaging experiment. The experimental plants were then left to grow for an additional 3 months in the greenhouse, during which time several aspects of host fitness were measured including: number of flowers, number of fruits, fruit weight, number of seeds in the oldest 3 fruits, and the proportion of germinable seeds collected from the oldest 3 fruits.

To assess leaf transcriptional responses to the above-described microbiome treatments, leaves were collected from each experimental plant for RNA extraction after the first and third inoculation. At both sampling time points, the experimental plants had been inoculated the day prior, incubated overnight in a high humidity misting chamber, returned to the greenhouse at 11am, and then sampled at noon. For leaf RNA sampling, four leaflets were excised from the plant, placed into two 15 ml plastic conical tubes, flash frozen in liquid nitrogen, and then transferred to the laboratory on dry ice and stored at -80° C until RNA extraction.

Examining microbiome generalism using a common garden experiment on novel host plants

To assay microbiome host generalism, we tested the hypothesis that microbiomes with a history of host swapping will more effectively colonize novel hosts and be more resilient to the effects of host filtering. Focusing on the host swapping lines, which all had last colonized tomato hosts, and the conspecifically passaged tomato lines, we inoculated each replicate line onto (i) tomato (*Solanum lycopersicum* var. moneymaker); a host with which the microbiomes share a history of association, as well as onto three novel hosts with no association history: (ii) canola (*Brassica napus* subsp. *napus*), (iii) sorghum (*Sorghum bicolor* var. BTx642), and (iv) corn (*Zea mays* convar. *saccharata* var. *rugosa*); a dicot and two monocots, respectively. The experiment involved a one-time inoculation of plants that were 3.5–4 weeks old. In total there were 6 replicates of each host/microbiome treatment (n = 96 plants). For example, each of the six host swapping pepper replicates was split four ways and inoculated onto a tomato, canola, sorghum, and a corn host plant. Additionally, 6 replicate control plants of each species (n = 24) were inoculated with sterile 10 mM $MgCl_2$, bringing the total plants for this experiment to 120. Each entire plant was harvested one week after inoculation and processed in the same way as the passaging experiment. The density of the microbial inocula and the subsequent leaf wash was assessed using both droplet digital PCR (ddPCR) and plate counts of colony forming units (CFUs) of leaf washings on KB agar plates.

DNA & RNA extraction, PCR, library preparation, and sequencing

To survey microbiome composition, DNA was extracted from every sample of each of the three above-described experiments. One sixth of the total leaf surface microbial community washed from each plant was used for DNA extraction with DNeasy Powersoil Kits (Qiagen). Sample order was randomized to avoid batch effects, and a blank (no sample) control was included in every round of DNA extraction. DNA concentration of each sample was quantified using the Qubit dsDNA HS Assay Kit. Sample DNA (10 μl) was used as template and PCR amplified for 35 cycles at the University of California - Davis Host Microbe Systems Biology Core using the 799F (5' – AACMGGATTAGATACCCKG – 3') - 1193R (5' – ACGTCATCCCCACCTTCC – 3') primer combination, which targets the V5-V7 region of the 16S rRNA gene, and was designed to minimize chloroplast amplification.[46,47] To further minimize host mitochondrial and chloroplast amplification, peptide nucleic acid (PNA) clamps were added to each reaction.[48] Resulting amplicons were diluted 8:1 and were further amplified for 9 cycles to add sample-specific barcodes, then quantified using Qubit, pooled in equal amounts, cleaned with magnetic beads and size selected via electrophoresis on a Pippin Prep gel (Sage Science, USA). The resultant library was then sequenced on the MiSeq (paired-end 300) platform (Illumina, USA).

To assess leaf transcriptional responses to microbiome inoculation in the specialization experiment, RNA was extracted from frozen leaf tissue using the Spectrum Plant Total RNA Kit (Merk/MilliporeSigma, MO, USA). Two tomato leaves from each sample

were powdered under liquid nitrogen in a sterile pestle and mortar. Following the manufacturer's instructions, 100 mg leaf powder was used for RNA extraction. RNA yields were quantified using the Qubit RNA High Sensitivity assay kit (ThermoFisher, USA). RNA samples were then sent to Novogene USA (Sacramento, CA) for quality control and library preparation, including Poly(A) capture, ligation-based addition of adapters and indexes, and multiplexing, followed by 150 bp paired-end sequencing on the Illumina NovaSeq6000 platform (Illumina, USA) to a depth of ~20M reads per sample.

QUANTIFICATION AND STATISTICAL ANALYSIS

Bacterial quantification using droplet digital PCR (ddPCR)

Foliar bacterial abundances of plant samples from the specialization and generalism common garden experiments were estimated using droplet digital PCR (ddPCR) on the Bio-Rad QX200 system (Bio-Rad, USA). We targeted the V5-V7 region of the 16S rRNA gene of cells in the leaf washings using the chloroplast-excluding 799 F (5′-AACMGGATTAGATACCCKG-3′)–1389R (5′ -ACGGGC GGTGTGTRC-3′) primer combination. Five microlitres of 1:10 diluted leaf wash was combined with 11 μl of 2× EvaGreen Supermix (Bio-Rad, USA) and 0.22 μl of each primer, and 5.56 μl of molecular grade water to a total volume of 20 μl. Reaction mixes were then loaded into the QX200 droplet generator with 70 μl of droplet generation oil and then transferred to a PCR plate. Thirty-nine cycles of PCR were performed under the following conditions: 95 °C for 10 min, 95 °C for 30 s, 55°C for 30 s, 72 °C for 2 min, with steps 2–4 repeated 39 times, 4 °C for 5 min, and 90 °C for 5 min. EvaGreen signal was measured on the QX200 droplet reader, cutoff thresholds were set for each column based on background fluorescence in no template controls, and concentrations were determined using the associated QuantaSoft software.

Sequence processing

16S rRNA gene amplicon sequences were processed using the DADA2 pipeline[49] implemented in the R statistical environment,[50] including the packages ShortRead,[51] Biostrings,[52] and Phyloseq.[53] Forward and reverse reads were truncated at 260 and 160 bp, respectively, and quality filtered using the function 'filterAndTrim' with default settings (i.e. maxN=0, maxEE=c(2,2), and truncQ=2). Error rates for forward and reverse reads were determined using the 'learnErrors' function, and then applied to remove sequencing errors from reads and assign them to amplicon sequence variants (ASVs) using the 'dada' function. Paired reads were merged, converted into a sequence table, and then chimeric sequences were removed from the sequence table. Taxonomy was assigned to the remaining ASVs using the 'assignTaxonomy' function, which implements the RDP Naïve Bayesian Classifier algorithm with kmer size 8 and 100 bootstrap replicates.[54] This taxonomic classification used the Silva (version 138) SSU taxonomic training dataset formatted for DADA2.[55] Chloroplast and mitochondrial sequences were filtered from the ASV table by removing any ASVs with a taxonomic assignment of 'Chloroplast' at the Order level or 'Mitochondria' at the Family level, respectively. Lastly, we applied the 'isContaminant' function (method = prevalence) from the package 'decontam'[56] to our samples using our blank (no sample) DNA extractions to identify and remove putative contaminants introduced during DNA extraction.

For the RNAseq dataset, sequence files were run through FastQC[57] to obtain sequence quality information. Sequence reads were mapped to the tomato (*S. lycopersicum* var. 'Fla.8924') genome from Alonge et al.,[58] downloaded from the Sol Genomics Network website.[59] We used STAR to map transcript reads to the genome[60] using runMode alignReads with quantMode set to GeneCounts to simultaneously perform counts of each read mapped to a gene.

Statistical Analysis

All statistical analyses were performed using R version 4.0.3.[50] Community matrices were rarefied to 13500 counts per sample ten times and averaged in order to account for differences in sampling extent across samples. The same rarefying procedure was performed for the specialization and generalism (common garden on novel hosts) experimental samples, but to a depth of 31800 and 7900 counts per sample, respectively. In all three cases, the depth to which we rarefied was sufficient to survey the standing diversity in all samples (Figures S6A–S6C). Bray Curtis bacterial community dissimilarities were calculated between samples using the 'vegdist' function in the vegan package.[61] Community structure differences among experimental passage (1–6), host species identity, transmission mode, experimental block, and a host species by transmission mode interaction were assessed using a PERMANOVA on Bray-Curtis distances using the 'adonis' function (also in the vegan package), which performs a sequential test of terms and uses the algorithm presented in Anderson.[62] The order of terms in the model for the passaging experiment was: passage, host, transmission mode, block, and host x transmission, with microbiome line ID specified as strata. The order of terms for the specialization experiment was previous host and experimental block, and for the generalism experiment it was host, previous host, and experimental block. In all cases term order did not impact qualitative conclusions. To assess the change in the relative strength of these factors through time, a PERMANOVA was performed for each of the six passage time points separately. In such instances of hypothesis testing on subsetted data, *p* values were adjusted for multiple comparisons using the Benjamini–Hochberg procedure with the 'p.adjust' function (method='hochberg') in the stats package in base R. Principle components analysis was performed on community ASV tables using the 'prcomp' function, with scale=F chosen.

To assess phylogenetic patterns in the phyllosphere communities, we constructed a phylogenetic tree of all ASVs in the community matrices of the three sequence datasets, which included 8395 ASVs. Sequences were aligned using the 'AlignSeqs' function in the DECIPHER package[63] using default settings. Next, pairwise distances between sequences were calculated using the 'dist.ml' function in the phangorn package version 2.5.5.[64] These distances were then used to construct a neighbor-joining tree using the 'NJ'

function in phangorn. Lastly, the neighbor-joining tree was used to create a generalized time-reversible with gamma rate variation (GTR+G+I) maximum likelihood tree using the 'pml', 'update', and 'optim.pml' functions in the phangorn package. We calculated the mean pairwise distance (MPD) of taxa in each sample and compared to the MPD of a community randomization null model (species.pool) to calculate the standardized effect size (SES) using the 'ses.mpd' function in the picante package.[65] Here a Z-score (the SES of MPD versus the null community) below zero is interpreted as phylogenetic clustering whereby co-occurring taxa are more closely related than taxa drawn at random from the species pool. Z-scores above zero, are taken to indicate phylogenetic overdispersion, where co-occurring taxa are more distantly related than the null expectation. While the use of the 16S rRNA gene for such phylogenetic analyses is reasonable considering it contains both conserved and variable regions, there are nevertheless limitations on our ability to capture functional and/or genomic differences among taxa, especially traits that have been acquired through horizontal gene transfer.

To examine patterns of microbiome network attributes we constructed co-occurrence networks from the community matrices after transforming counts to presence/absence. The function rcorr in the HMisc package[66] was used to generate a Pearson's correlation matrix with corresponding *p*-values. Following Benjamini-Hochberg correction for multiple comparisons (false discovery rate <0.1), a network was constructed on significant correlations using the igraph package,[67] following the procedure described in Debray et al.[68] To obtain 95% confidence intervals for the network attributes of interest we developed a bootstrapping approach whereby the community was rarefied and the community networks were computed and summarized following the above-described methodology iteratively 100 times.

For univariate data including ASV-level richness, MPD SES, and abundance data, a linear mixed effects model was fit to test for significant effects of the passage, host, transmission mode, and block, with interactions therein with sample ID as a random effect using the package lmrTest.[69]

Relative abundance across the complete set of ASVs across plants and transmission groups at the sixth passage for each host plant shows a considerable number of zeros (Figure S1, columns 1 & 3). Accordingly, we use a presence/absence model framing to identify taxa that differentially establish under the different transmission treatments. The presence/absence models include a random effect reflecting plant to account for non-independence among observations due to the sampling design. Since we are specifically interested in whether some ASVs were more likely to establish under different transmission modes, we included ASV as a crossed random effect among transmission groups. All models were fitted using the brms package in R,[70] with the full model defined as: $y \sim (\text{trans.type}|\text{ASV}) + (1|\text{plant})$, using a binomial distribution and logistic regression for presence/absence. The first term is the focal estimate of how transmission mode varies by ASV, and the second term corrects for the fact that different plants may be differently permissive. See Figures S7A and S7B for details of model convergence and fit.

To examine whether microbiome treatment in the specialization experiment elicited tomato leaf transcriptional responses, we performed differential expression analysis on the concatenated RNAseq read counts. This involved using edgeR[71] to perform a genewise negative binomial generalized linear model with quasi-likelihood test (glmQLFTest) on all pairwise comparisons involving the tomato microbiome, using a false discovery rate of 0.05. Finally, to visualize transcriptional responses among microbiome treatments, principle components analysis was performed on normalized (counts per million) read counts and a linear mixed effects model was performed on PCs 1 and 2 with time point and microbiome treatment as fixed effects and sample ID as a random effect.